Available online at www.sciencedirect.com
SCIENCE DIRECT
Wear 260 (2006) 1136–1144
WEAR
www.elsevier.com/locate/wear

Measuring the dynamic forces to identify the friction of a graphite–copper contact for variable temperature and current

Janko Slavič, Miha Boltežar *

Aškerčeva 6, Faculty of Mechanical Engineering, University of Ljubljana, 1000 Ljubljana, Slovenia

Received 16 November 2004; received in revised form 18 July 2005; accepted 28 July 2005
Available online 1 September 2005

Abstract

In this paper we present experimental and analytical techniques for identifying the coefficient of friction (COF) of a graphite electric brush sliding against a commutator for different contact temperatures and electric current densities. A direct measurement of the instantaneous dynamic forces is used to identify the coefficient of friction. The experimental example shows that the presented procedures can be used to determine the optimum operating ranges for the temperature and the electric current density.

Keywords: Coefficient of friction; Graphite; Copper; Electric current; Heat; Temperature; Brush

1. Introduction

Despite the fact that electric brushes have been integral parts of electric motors for decades, reducing the coefficient of friction (COF) of the electric brushes remains a challenge. The reason why the COF has proved to be such a problem is the complexity of the different phenomena, e.g., electric, thermal, elasto-mechanic and chemical. In the next paragraphs we will take a brief look at some of the research work carried out over the past decade.

Milkovič and Ban have done a lot of experimental work on the subject of the COF [1,2]. They found that the pulsating current supply of the commutator machine has a noticeable effect on the size of the contact area between the electric brush and the commutator. Using the "electric-balance" method they found that an increase in the amplitude of the pulsating current leads to a decrease in the COF. In their research [1,2] a short-circuited commutator was used, and only the lateral force was measured.

The research work of Milkovič et al. was continued by Šimunič et al. [3] who built a mathematical model of the COF for dc machines supplied with a pulsating current. They found that the temperature T decreases the COF at a rate $\approx -8 \times 10^{-3}\sqrt{T}$; the average current I, at a rate $\approx -3 \times 10^{-4} I$; and the maximum current I_m, at a rate $\approx -1.5 \times 10^{-4} I_m$. The frequency of the pulsating current was found to have only a negligible effect.

Csapo et al. [4] measured the COF of a graphite–graphite electric contact in the presence of argon. They found that in argon gas and at low sliding speeds the COF can be as low as 0.06; however, as the sliding speed increases the COF increases up to 0.7. They found that the electric current passing through the contact area increases the COF. Using a strain gauge they measured only the lateral force; the influence of the temperature was not studied.

Mansori et al. [5] studied steel/graphite sliding contacts crossed by a dc electric current and subjected to a dc magnetic field. They found that the combined effects of the electric current and the magnetic field reduced the COF. The experimental set up is a modification of that from [4]; the electric current was up to 80 A and the magnetic field intensity was up to 6×10^4 A m^{-1}.

They found that the electric current effectively decreased the COF, and that the COF can be further reduced with a magnetic field intensity higher than $\approx 2 \times 10^4$ A m^{-1}.

* Corresponding author. Tel.: +386 1 4771 608; fax: +386 1 2518 567.
E-mail address: miha.boltezar@fs.uni-lj.si (M. Boltežar).

0043-1648/$ – see front matter © 2005 Elsevier B.V. All rights reserved.
doi:10.1016/j.wear.2005.07.016

In [6] Senouci et al. studied the wear mechanism of a graphite–copper electric sliding contact. They found that the mechanical wear increased with the applied normal load and decreased depending on the basal plane orientation of the graphite. However, on the other hand, the electrical wear decreased with the applied normal load and decreased when the graphite's basal plane was oriented in the sliding direction. For the testing they used a classic pin-on-disk tribometer in a controled gas environment. They found the COF decreased when an electric current was applied. Furthermore, they observed a small difference in the COF between the cathode and anode brush (≈15% higher on the cathode).

In 2001 Zhao et al. [7] published their research on the influence of the sliding speed, the normal load and the current on the COF and the wear of a carbon–graphite material. They used a classical pin-on-disc measurement where the normal force was applied through a spring, and only the lateral force was measured. The study showed that without an electric current the effect of the load and the sliding speed on the wear rate can be described by Archards wear equation ($W = KNl/H$, where N is the normal contact force, l is the sliding length, H is the material's hardness and K is the wear coefficient) [8]. However, when applying the current the friction and wear behaviors are both complicated and difficult to describe. Nevertheless, using scanning electron microscopy (SEM) to analyze the wear particles from the tests with and without an electric current the different wear processes were identified.

Using experimental and theoretical techniques Bryant and coworkers [9–12] found that the performance of an electric brush is greatly affected by the combined effects of the current flow and the sliding. Using the finite-element method Lu and Bryant [11,12] simulated a carbon–graphite block sliding against a fast moving conductor. To simulate the coupled electrical, thermal and thermo-elastical fields and the elastic contact stresses they took into account the heating due to frictional power dissipation and the internal Joule heating.

The simulations showed that the real contact area between the brush and the slip ring is only a small fraction of the apparent contact area; therefore, the electric current is constricted and consequently the Joule heating increases. In combination with the increased frictional heating the local temperatures can be extremely high. As a consequence of local temperature peaks the material locally expands and separates the brush and the slip ring at the remaining contact spots. The result is that even more current goes to the locally heated contact spot, which leads to thermo-elastic instabilities or thermal mounding [9,13]. Bryant et al. found good agreement between the experiment and the theoretical models, and they also found that even though the thermal mounds might appear only intermittently, they can still induce a severe wear rate [14].

Further work of Bryant et al. [15] revealed that the thermal mounds can be reduced by the surface waviness that induces (rocking) vibrations. The two main functions of the rocking vibrations are (a) to prevent stationary spots (in time) that could lead to thermal mounds, and (b) to create a gap through which the particles can escape without scratching the brush's bottom surface. They found that micro-vibrations with a 10–100 μm amplitude and 10–100 Hz can reduce the sliding wear by up to 50% (mass of brush under experiment: ≈90 g). Using SEM they discovered that the typical characteristic length of the wear particles decreased in the rocking regime. By studying the effects of the clearance between the carbon brush and the holder they found that tighter fits restricted the rocking and looser fits permitted it; this holds regardless of the tangential or axial clearance. Severe vibrations can however encourage arching of the brushes and also increase the wear [16].

The dynamics of the electric brush and the rocking phenomena were further studied in [17], where a quantitative relationship between the amount of wear and the total kinetic energy of vibration was observed. In recent studies [18] a mathematical model with 4 degrees of freedom was studied.

It is usually hard to distinguish thermal mounds from sparking, and the reasons for sparking are usually the sharp peaks in the electric current that are a result of the commutation. From the electrical point of view the magnetomotive force, which is derived from the commutation's rectifying current, generated a harmonic magnetic flux; this waveform represents a higher amplitude of the reactance voltage, which was found to be the main cause of the spark generation [19].

Using ultra-high-speed photography (up to 800,000 frames/s) Hanazawa et al. [20] optically observed that the commutation spark is generated at the moment when the brush and the commutator segment (lamella) are separated from each other during the rotation. They measured the lifetime of the spark and found that spark initiation is observed at the instant of the current peak. The spark then gradually grows for ≈60 μs, and then annihilates in the next ≈180 μs. Because the spark's lifetime is considerably shorter then the time needed for building up the thermal mound (100–200 ms [12]) sparking can lead to thermal mounding only if it is continuous. However, thermal mounds can also build up because of friction and other effects.

Research into commutator wear and its wave characteristic was also done by Wilk and Moson [21]. They found that the wear changed in such a way that the top of the profiles of the waviness always moved in the opposite direction to the commutator's rotation. This could lead to the conclusion that the lamellas are also worn out on the lead-out side of the brush (as are the brushes).

In the field of measuring the coefficient of friction under dynamic conditions a lot of research was done by Polycarpou and Soom [22–24]. Polycarpou and Soom [22] used piezoelectric force sensors to identify the coefficient of friction. In this research a similar procedure will be used; however, more attention is paid to the actually measured dynamic forces.

Friction-induced vibrations were also widely studied by Akay and coworkers [25–27].

Some very recent atomic-scale research by Dienwiebel et al. [28] on the topic of the superlubricity of graphite crystals is very promising. By measuring the atomic-scale friction as a

function of the rotation angle of a graphite mono-crystal they found a region of COF decrease of more than one order of magnitude. Further experimental work on the topic of superlubricity [29] revealed that the reason for the ultra-low friction could be the transition from stick-slip phenomena (with the periodicity of the graphite hexagonal crystal lattice) to continuous sliding.

We would like to point out that researchers working on different size scales observed a decrease of the COF of graphite as a consequence of dynamic instabilities [15,28,29]. This is probably because they observed the same phenomena that was already studied by Oden and coworkers [30,31], who found that the well-known reduction in the COF with an increase in sliding speed is a consequence of the dynamic instability of stick-slip phenomena on the atomic scale. This dynamic instability was experimentally proven and theoretically explained by Dweib and D'Souza [32,33].

The aim of our work was to study the COF properties of an electric brush and copper commutator couple. While other researchers have focused on the long-term COF, this study was focused on the changes in the instantaneous COF while varying the temperature and the current density. Furthermore, while other researchers measured the COF of the brush indirectly by measuring the force of the brush on the brush-holder, this research presents a direct measurement of the forces acting on the brush.

2. Experimental setup

A scheme of the experimental setup is shown in Fig. 1. The surface of the short-circuited commutator is connected to two electric circuits. The primary electrical circuit involves a 12.5 V dc source that is connected in series to a variable resistance with the electric brush tip as a switch. The primary electrical circuit is used to vary the electric current through the contact area between the brush tip and the commutator. The approximately 6 mm × 11 mm contact area of the additional 3 g brush and the 4 N force guarantee a disconnects- and arcs-free contact, Fig. 1.

The second electrical circuit with a power-variable ac source is used for Joule heating of the commutator only.

No interference between the two electrical circuits could be observed.

As shown in Fig. 1, one electric brush of the primary circuit is attached to a three-axis forcemeter (Kistler 9017 A); the forcemeter is further attached to rigid surroundings. The surroundings of the rotor and forcemeter are electrically and mechanically insulated.

The piezo-electric forcemeter measures three orthogonal forces simultaneously; in this study x, y and z. The dynamic range of the forcemeter is as follows: $F_z = -2$ to $+2$ kN and $F_x = F_y = -1$ to $+1$ kN. The threshold of the sensor is <0.01 N.

The forcemeter is connected to a conditioning amplifier, of which the high-pass filter (characteristic time constant) defines the lowest frequency that can be measured.

The Brüel&Kjær Nexus 2692 conditioning amplifier with high-pass filter was set to the lowest possible value, i.e., 0.1 Hz. Because of the high-pass filter only dynamic forces can be measured. To denote the dynamic forces the subscript "d" is used, see Fig. 2.

Consequently, with the high-pass filter, the static pre-stress forces, denoted with the subscript "s", cannot be measured with this set-up. As we will see later, it is also not needed.

The dynamic forces and the voltage of the first electric circuit were acquired simultaneously with a 16 bit A/D National Instruments acquisition card (sampling frequency: 1 kHz).

To ensure a good contact, the actual contact force (=static + dynamic) between the brush tip and the commutator must be positive. This condition ensures the static pre-stress force is equal to or higher than the maximum negative dynamic force.

The actually used static pre-stress forces are estimated to be in the range 2–3 N.

The tested commutator is made up of 24 lamellas with an outer diameter of approximately 22 mm, the rotating speed

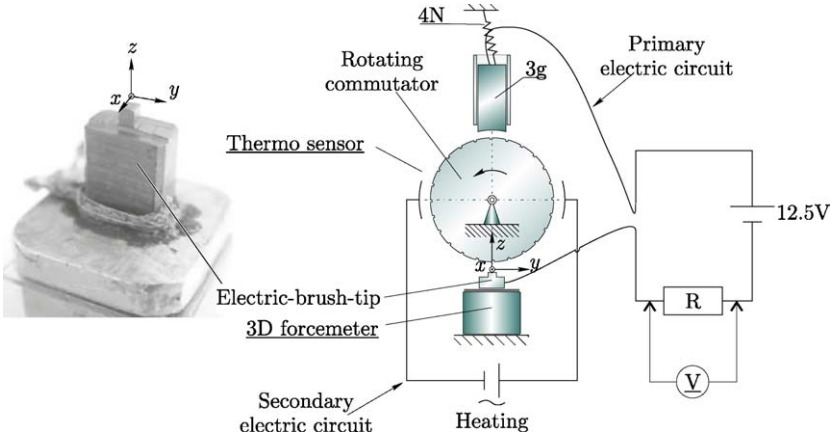

Fig. 1. Scheme of the experimenal setup. Measured values are underlined.

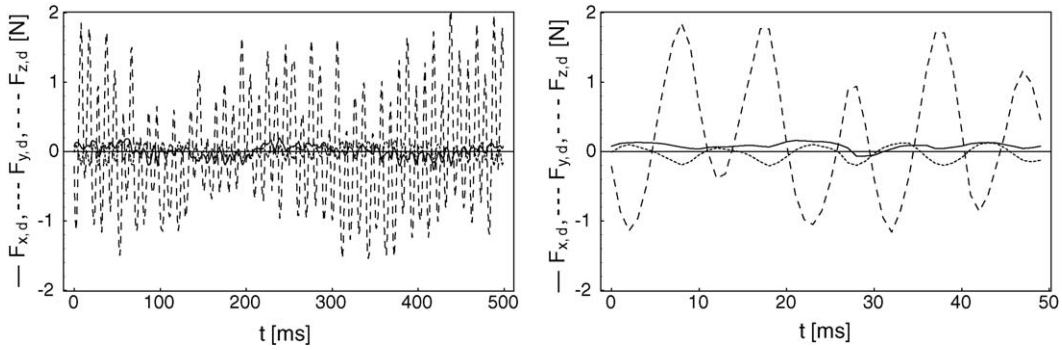

Fig. 2. Dynamic forces on the brush at a rotating speed ≈250 rpm.

of the commutator is 250 revolutions per minute (rpm); the sliding speed of the brush is approximately 0.28 m/s.

To achieve a well-defined electro-mechanical contact, two brush tips are used: *tip* (*a*) a flat-shaped cross-section 2 mm × 2 mm with a length of 2 mm, and *tip* (*b*) a flat-shaped cross-section 1 mm × 1 mm with a length of 1 mm. As will be seen later, the dynamic normal force ranges from approx. −2 N to +2 N; if a 2 N static force is assumed, then the approximately 4 N of normal direction is expected; the maximum contact pressure of the smaller brush tip is 4 N/1 mm^2 = 4 MPa, and for the second brush tip the maximum contact pressure is 4 N/4 mm^2 = 1 MPa.

The main reason for using a brush tip with a relatively small cross-section is to achieve a quick run-in period and also to achieve a well-defined a-spot (or cluster of a-spots) electrical contact [34,35].

The commutator's surface temperature is measured using a contact thermo-sensor, while the rotor is at rest; this measurement takes about 5 s.

3. Identifying the coefficient of friction

3.1. Correlation between the x, y and z forces

In the introduction we cited several authors, most of them measured only the normal and the tangential force on the brush, as they expected the axial force to be negligible [22].

By using the correlation function we will quantitatively show that the influence of the force in the axial direction (*x*) is actually negligible.

The correlation function of discrete lists *x* and *y* is defined by:

$$C_{x,y}(j) = \frac{\sum_i (x_i - \bar{x})(y_{i+j} - \bar{y})}{\sqrt{\sum_i (x_i - \bar{x})^2}\sqrt{\sum_i (y_{i+j} - \bar{y})^2}} \quad (1)$$

At $j = 0$ or $\tau = 0$ s the correlation function equals the Pearson's correlation coefficient [36]. Figs. 3–5 present correlation functions for typical measured dynamic forces. We can see that the correlation functions are influenced by two frequencies: the rotating speed (f_0) and the rotating speed

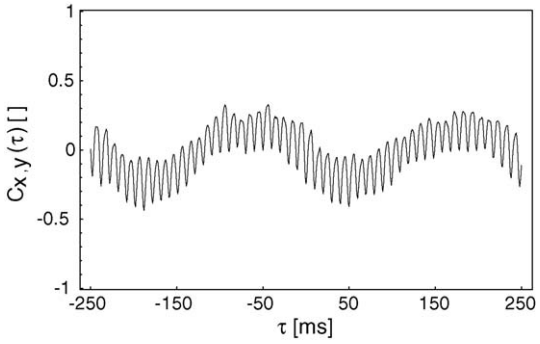

Fig. 3. Correlation function between the dynamic forces $F_{x,d}$ and $F_{y,d}$ as a function of time shift τ (1).

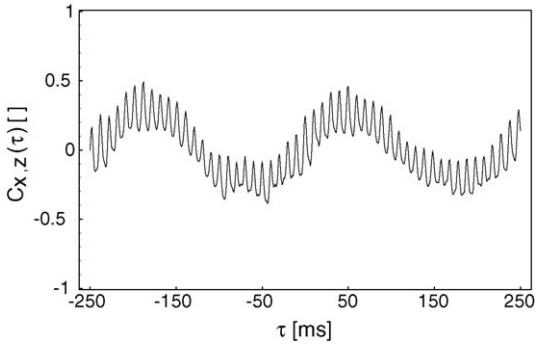

Fig. 4. Correlation function between the dynamic forces $F_{x,d}$ and $F_{z,d}$ as a function of time shift τ (1).

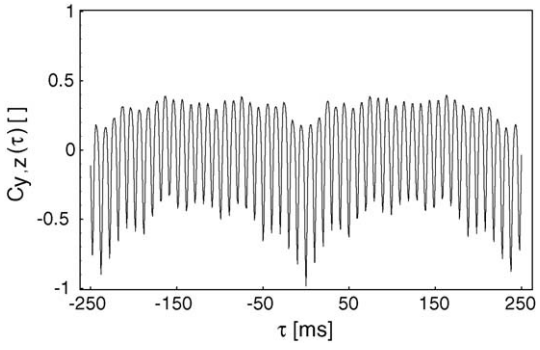

Fig. 5. Correlation function between the dynamic forces $F_{y,d}$ and $F_{z,d}$ as a function of time shift τ, Eq. (1).

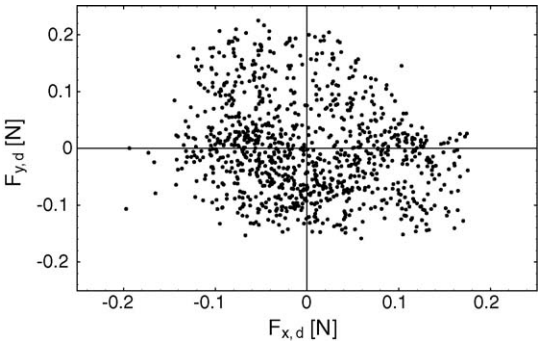

Fig. 6. Force phase-plots of forces $F_{x,d}$ and $F_{y,d}$.

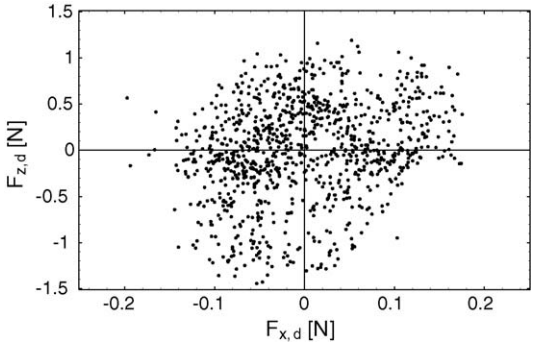

Fig. 7. Force phase-plots of forces $F_{x,d}$ and $F_{z,d}$.

multiplied by the number of lamellas (f_l). By using the cross-spectra it was found that at f_l the amplitudes of the cross-spectra yz are considerably higher than the amplitudes of the cross-spectra xy and xz at the same frequency.

From Fig. 5 it is obvious that at zero time-shift ($\tau = 0$ ms) the correlation yz is close to -1 (negative because of the orientation of the forcemeter).

We have experimentally observed that the assumption of negligible axial forces can be used if the correlation yz is high, we found $|C_{y,z}| \gtrsim 0.85$ as a necessary, but not sufficient, condition. All the measurements in this paper are in agreement with this condition.

As the COF is very dependent on the commutator surface, the position of the brush relative to the commutator (all three translations and all three rotations), a well run-in brush, the rotor's turning speed, the length of the brush tip, a good arrangement of the bearings and rotor, etc., we found that the simple Pearson's correlation coefficient was suitable for a quick assessment of a potentially good measurement.

3.2. Using linear regression to identify the coefficient of friction

The Coulomb friction law is defined by:

$$F_t = \mu F_n, \tag{2}$$

where μ is the COF and F_t and F_n are the tangential and normal forces, respectively. Because the axial force is negligible, the following can be used:

$$F_y = \mu F_z, \tag{3}$$

In our case the contact force F_z is defined as the sum of the static pre-stress and the measured dynamic force: $F_z = F_{z,s} + F_{z,d}$ (Figs. 6 and 7). By using the same principle for the friction force in Eq. (3):

$$F_{y,s} + F_{y,d} = \mu(F_{z,s} + F_{z,d}) \tag{4}$$

and further, by using $F_{y,s} = \mu F_{z,s}$, we see that only the dynamic forces are needed to identify the COF:

$$F_{y,d} = \mu F_{z,d}. \tag{5}$$

Eq. (5) is valid if the coefficient of friction does not depend on the magnitude of the normal force. The validity dependence of the COF on the normal force will be researched later.

Fig. 8 presents the phase-plot of the forces $F_{y,d}$ and $F_{z,d}$. By using linear regression we can find the COF that best suits the measured data:

$$E = \sum_i^n (F_{y,d,i} - f(F_{z,d,i}))^2, \tag{6}$$

where:

$$f(F_z) = \mu_r F_z + F_{y,0}. \tag{7}$$

By minimizing Eq. (6) according to μ_r and $F_{y,0}$ we find:

$$E = -\frac{-\sum_i F_{y,d,i} \sum_i F_{z,d,i} + n \sum_i F_{y,d,i} F_{z,d,i}}{(\sum_i F_{z,d,i})^2 - n \sum_i F_{z,d,i}^2}. \tag{8}$$

The $F_{y,0}$ is not defined here, but it was found to be close to zero for all measurements.

Index τ is used to distinguish the linear regression COF from the theoretical μ.

3.3. Does coefficient of friction depend on normal force?

In Section 3.2 we used the usual assumption that the COF does not depend on the normal force. In this section measured data will be used to present methods for estimating

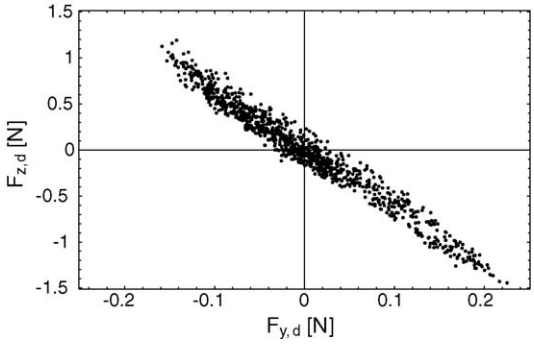

Fig. 8. Force phase-plots of forces $F_{y,d}$ and $F_{z,d}$.

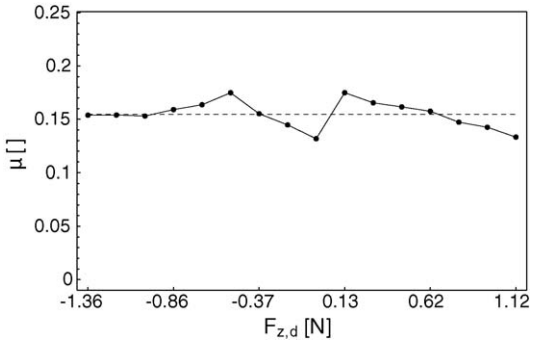

Fig. 9. Coefficient of friction as a function of $F_{z,d}$. (- - -) μ_r linear regression method, Eq. (8).

the influence of the amplitude of the normal force on the COF.

In the first step the measured dynamic forces are re-sorted according to the normal force $F_{z,d}$ into 16 ranges from −1.36 to +1.12 N. In the second step Eq. (5) is used to obtain an average COF in each range.

The results are presented in Fig. 9, we see that the COF differs by less than 15%. In the ranges where the force $F_{z,d}$ is near zero – because of dividing by small numbers (5) – a higher numerical error is present.

To decrease the division error we exclude the data with $F_{z,d}$ in the range −0.35 to +0.35 N.[1] The mean COF at negative dynamic forces (from −1.36 to −0.35 N) would be $\mu_a = 0.160$. Similarly, the COF at positive dynamic forces (from +0.35 to +1.12 N) would be $\mu_b = 0.155$.

A similar analysis for the COF's normal force was done for each measurement and will be commented on in Section 4.

4. Results and discussion

4.1. Temperature dependency of the COF

To measure the COF's dependency on temperature a secondary electric circuit is used (Fig. 1) to heat (Joule heating) the short-circuited commutator surface up to some particular temperature. It can be assumed that the brush tip in the contact zone is at a comparable average temperature to the commutator surface. The sliding velocity was 0.28 m/s and the normal force on the pin was in the range from 2 to 6 N. Compared to the heating energy (estimation 10–60 W) the dissipation of the friction energy (approximately 0.1 W) had a negligible influence on the average contact temperature.

The temperature test was made using the brush tip with the 2 mm × 2 mm cross-section; the rotating speed of the rotor was 250 rpm. After each 10 s a measurement of 2 s was acquired. The surface temperature of the commutator was measured only intermittently every 100–200 s; to measure the temperature the rotor needed to be stopped for a few seconds (denoted with symbol △ in Fig. 10).

In Fig. 10 the results of a 4060 s long experiment are shown. The test starts at 155 °C; we can see that the COF slowly decreased to a COF of approximately 0.1. However, at 1000 s, as the heating is increased, the temperature increased up to 175 °C, and in the same time the COF increased from 0.1 up to approximately 0.15. As at approximately 2000 s the heating decreased the COF decreased again to a level of approximately 0.1. At approximately 3600 s the temperature of the commutator surface decreased from 135 °C to approximately 130 °C, and consequently the COF increased. At approximately 3700 s the slightly increased heating raised the temperature to 135 °C, as a consequence the COF decreased again to 0.1. At the end of the experiment at 3950 s the heating was turned off and the temperature of the commutator surface fell in approximately 1 min from 135 to 100 °C, at the same time the COF increased from 0.1 to above 0.2.

From Fig. 10 we can also see that at high temperatures the COF increases slightly with normal force: μ_a is approximately 10% lower and μ_b is approximately 10% higher than the "average" μ_r. In the temperature range below 155 °C the difference between μ_a and μ_b is much smaller and according to Section 3.3 the COF identified by linear regression μ_r is more accurate then in the region of high temperature (above 155 °C).

From the COF-versus-time and temperature-versus-time diagrams we can draw a COF–temperature diagram, see Fig. 11. As the temperature increases from 160 to 175 °C the COF increases, and later when the temperature decreases again the COF decreases also. However, as the contact zone needs time to revitalize we can observe a hysteresis during the cooling down. At about 130 °C the COF tends to increase steeply. According to Shobert [16] the evaporation of adsorbed water films on the commutator surface could be the reason for the friction reduction. As the glass-transition of the electric brush material is at approximately 120–130 °C, the reason for the abrupt decrease of the COF could be in the change of the mechanical properties and the contact dynamics [29].

4.2. Current density dependency of COF

To measure the COF's dependency on current density the brush tip with the 1 mm × 1 mm cross-section was used. The smaller cross-section makes it possible to achieve good contact situations and high current densities. To simulate the working conditions of the commutator-brush couple the commutator surface was heated with the secondary electrical circuit to 100 °C. The rotating speed was 250 rpm, each 10 s a 2 s long measurement was made. The test duration was 700 s and the current density was increased step-wise from ≈2 A/mm^2 up to ≈6.5 A/mm^2, see Fig. 12.

In Fig. 12 we can see that as the current density increases the COF decreases. It is interesting that the current density

[1] For identifying the range the standard deviation of all samples can be used.

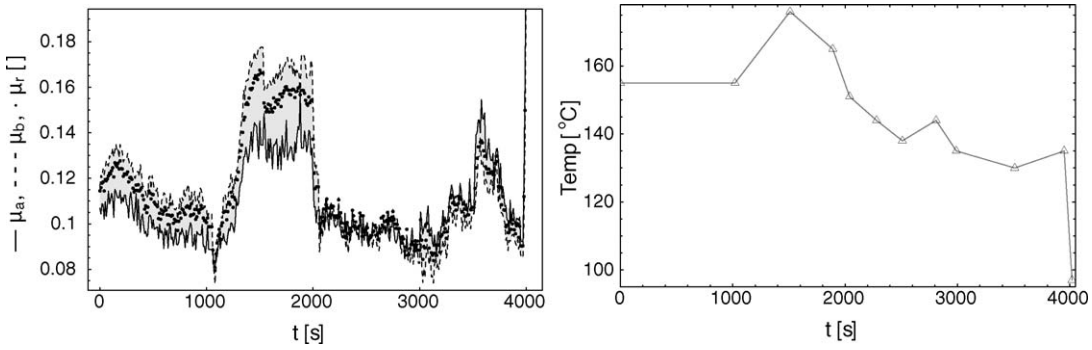

Fig. 10. COF and temperature in time.

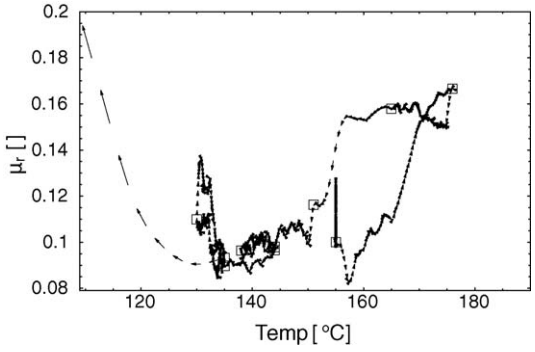

Fig. 11. COF as a function of temperature.

below 3.4 A/mm^2 has little effect on the COF. However, when the current density is increased at 290 s to 3.4 A/mm^2 the COF decreased very quickly. A similarly quick decrease can be observed when the current density is set to 4.5 A/mm^2 when the COF reaches a minimum of approximately 0.1. If the current density is increased even more, then the COF increases steeply up to 0.25; in a matter of a second sparking appears and the contact-zone is burned out and finally the contact is lost.

By comparing the results of the influence of the temperature and the current density we can see that there is a temperature- and current-density-dependent optimum range with a low COF. From the results it is believed that for a low COF it is very important that the contact-zone temperature is over the glass-transition temperature, but it should also be below the temperature at which the bonding materials of the graphite brush begin to burn out.

The surface temperature of the commutator could be measured only at the beginning and at the end of the test. Because of the current in the primary electrical circuit the temperature of the commutator surface rose from 100 °C at start up to 135 °C at the end (700 s); the real contact temperature of the contact-zone was probably higher. We believe that the current density changes the temperature of the contact zone and that this changes the friction.

5. Conclusions

To identify the coefficient of friction other researchers usually measure only the tangential force, while the normal force is determined by the compression of the spring. Because the tangential forces are measured on the brush holder the unilateral contacts between the brush and the brush holder are not excluded, and consequently only the average tangential forces can be measured.

In contrast to classical research this study presents a direct measurement of the friction forces. As the electric brush was attached to a forcemeter that was attached to rigid surroundings we were able to directly measure the instantaneous dynamic forces applied to the brush. With a direct measurement of the dynamic forces it is possible to measure relatively

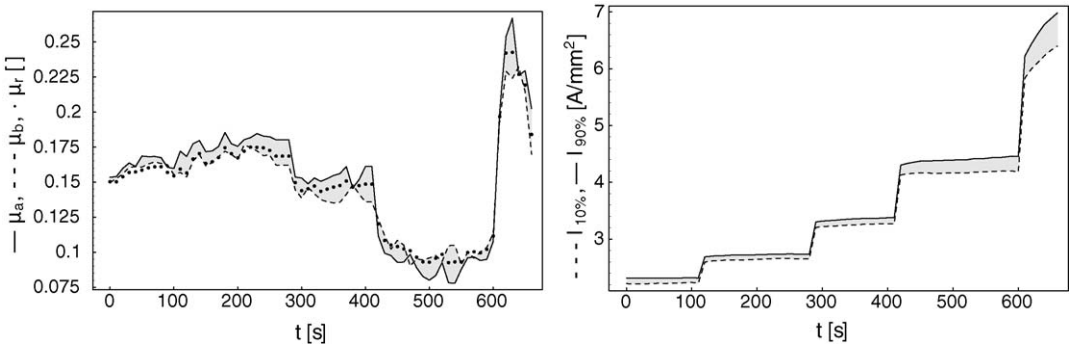

Fig. 12. COF and current density of the first electrical circuit.

quickly the changes of the COF with temperature or current density. Furthermore, by measuring the instantaneous forces we were able to experimentally show that the COF under optimum conditions is relatively constant with the normal force; however, at increased temperatures, i.e., at a high COF, we observed a slight increase of the COF as the normal force increases.

The proposed measurement and analysis techniques for the temperature and the current-density-dependent identification of the COF are presented for an example of a graphite brush. To achieve a dynamically stable friction regime, and also a low amount of frictional energy, it is better to use relatively low rotating speeds. The Pearson's correlation coefficient was found to be very useful for determining the quality of the measurement.

It was experimentally observed that the COF of the analyzed electric brush is highly temperature dependent, with an optimum temperature range approximately 30 °C wide (above the glass-transition temperature). The influence of the current density was also found to have an optimum range: by increasing the current density the COF decreases to an optimum level, and beyond that level of current density the COF decreases sharply and sparking occurs. We believe that the a-spot in the contact with the commutator locally warms to a temperature above the glass-transition temperature of the electric-brush; if the current density is, however, increased further the a-spot becomes thermally unstable and the temperature of the a-spot increases rapidly to the melting point [9,10,13].

A current density of approximately 6 A/mm^2 was found to cause thermal instabilities and break the contact point. This finding is in agreement with the numerical simulations of Lu and Bryant [12] who numerically simulated a thermally insulated brush and found that a current density at ≈2–3 A/mm^2 led to thermal instabilities.

The proposed techniques are presented for a specific graphite-based electric brush, but they can easily be applied to other materials. With the proposed techniques for a given electric brush the optimum temperature and current-density conditions can be determined.

References

[1] M. Milković, Test methods and measuring apparatus for measurement of the dynamic coefficient of friction of brushes, Carbon 30 (4) (1992) 587–592.

[2] M. Milković, D. Ban, Influence of the pulsating current amplitude on the dynamic friction coefficient of electrographite brushes, Carbon 34 (10) (1996) 1207–1214.

[3] Z. Šimunić, M. Milkovic, Mathematical-model of the coefficient of friction of brushes on dc machines supplied by pulsating current, Carbon 31 (7) (1993) 1019–1029.

[4] E. Csapo, H. Zaidi, D. Paulmier, Friction behaviour of a graphite–graphite dynamic electric contact in the presence of argon, Wear 192 (1–2) (1999) 151–156.

[5] M. Mansori, D. Paulmier, J. Ginsztler, M. Horvath, Lubrication mechanisms of a sliding contact by simultaneous action of electric current and magnetic field, Wear 225–229 (1999) 1011–1016 (Part 2).

[6] A. Senouci, J. Frene, H. Zaidi, Wear mechanism in graphite–copper electrical sliding contact, Wear 225–229 (1999) 949–953 (Part 2).

[7] H. Zhao, G. Barberb, J. Liuc, Friction and wear in high speed sliding with and without electrical current, Wear 249 (5–6) (2001) 409–414.

[8] J. Archard, Contacts and rubbing of flat surfaces, J. Appl. Phys. 24 (1953) 981.

[9] M. Bryant, Y. Yune, Electrically and frictionally derived mound temperatures in carbon graphite brushes, IEEE Trans. Components Hybrids Manuf. Technol. 12 (1989) 229–235.

[10] M. Bryant, A particle ejection mechanism for brushwear, IEEE Trans. Components Hybrids Manuf. Technol. 14 (1991) 71–78.

[11] C. Lu, Thermal and mechanical behavior and failure of carbon and metal-graphite brushes in sliding electrical contacts, Ph.D. thesis, The University of Texas, Austin, 1993.

[12] C. Lu, M. Bryant, Thermal mounding in high speed dry sliders: experiment, theory and comparison, Wear 174 (1–2) (1994) 137–146.

[13] L. Afferrante, M. Ciavarella, Instability of thermoelastic contact for two half-planes sliding out-of-plane with contact resistance and frictional heating, J. Mech. Phys. Solids 52 (7) (2004) 1527–1547.

[14] M. Bryant, J. Wang, J. Lin, Thermal mounding in high speed dry sliders: experiment, theory and comparison, Wear 181–183 (1995) 668–677.

[15] M. Bryant, A. Tewari, D. York, Effects of micro (rocking) vibrations and surface waviness on wear and wear debris, Wear 216 (1) (1998) 60–69.

[16] E. Shobert, Carbon Brushes; the Physics and Chemistry of Sliding Contacts, Chemical Publishing Company Inc., New York, NY, 1965.

[17] M. Bryant, D. York, Measurements and correlations of slider vibrations and wear, J. Tribol. Trans. ASME 122 (1) (2000) 374–380.

[18] C. Pholsiri, M. Bryant, Vibrations of a four-degree-of-freedom rigid body sliding against a wavy surface, J. Sound Vib. 235 (5) (2000) 763–786.

[19] T. Hanazawa, T. Egashira, Y. Tanaka, J. Egoshi, Ultrahigh- and high-speed photography and image-based motion measurement, in: Proceedings of SPIE, vol. 3173, The International Society for Optical Engineering, San Diego, California, 1997, pp. 115–122.

[20] T. Hanazawa, A. Almazroui, T. Egashira, Unraveling the image of commutation spark generated in universal motor, IEEJ Trans. IA 123 (10) (2003) 1161–1168 (in Japanese, partly in English).

[21] A. Wilk, I. Moson, The wave character of commutator wear in electrical machines, Wear 253 (9–10) (2002) 935–945.

[22] A.A. Polycarpou, A. Soom, Application of a two-dimensional model of continuous sliding friction to stick-slip, Wear 181–183 (1) (1995) 32–41.

[23] A.A. Polycarpou, A. Soom, Boundary and mixed friction in the presence of dynamic normal loads. 1. System model, J. Tribol. Trans. ASME 117 (2) (1995) 255–260.

[24] A.A. Polycarpou, A. Soom, Boundary and mixed friction in the presence of dynamic normal loads. 2. Friction transients, J. Tribol. Trans. ASME 117 (2) (1995) 261–266.

[25] M. Bengisu, A. Akay, Stability of friction-induced vibrations in multi-degree-of-freedom systems, J. Sound Vib. 171 (4) (1994) 557–570.

[26] J. Swayze, A. Akay, Effects of system dynamics on friction-induced oscillations, J. Sound Vib. 173 (5) (1994) 599–609.

[27] M. Bengisu, A. Akay, Relation of dry-friction to surface roughness, J. Tribol. Trans. ASME 119 (1) (1997) 18–25.

[28] M. Dienwiebel, G.S. Verhoeven, N. Pradeep, J.W.M. Frenken, J.A. Heimberg, H.W. Zandbergen, Superlubricity of graphite, Phys. Rev. Lett. 92 (12) (2004) (art. no. 126101).

[29] A. Socoliuc, R. Bennewitz, E. Gnecco, E. Meyer, Transition from stick-slip to continuous sliding in atomic friction: entering a new regime of ultralow friction, Phys. Rev. Lett. 92 (12) (2004) (art. no. 134301).

[30] J. Oden, J. Martins, Models and computational methods for dynamic friction phenomena, Comput. Methods Appl. Mech. Eng. 52 (1–3) (1985) 527–634.
[31] J. Martins, J. Oden, F. Simoes, Recent advances in engineering science—a study of static and kinetic friction, Int. J. Eng. Sci. 28 (1) (1990) 29–92.
[32] A. Dweib, A. D'souza, Self-excited vibrations induced by dry friction, part 1: Experimental-study, J. Sound Vib. 137 (2) (1990) 163–175.
[33] A. D'Souza, A. Dweib, Self-excited vibrations induced by dry friction, part 2: Stability and limit-cycle analysis, J. Sound Vib. 137 (2) (1990) 177–190.
[34] R. Holm, Electric Contacts, fourth ed., Springer-Verlag, 1967.
[35] P. Slade (Ed.), Electrical Contacts: Principles and Applications, Marcel Dekker, 1999.
[36] E. Weisstein, CRC Concise Encyclopedia of Mathematics, second ed., Chapman & Hall/CRC, 2002.